



HAL
open science

Microstructure effects on transverse cracking in composite laminae by DEM

Yong Sheng, Dongmin Yang, Yuanqiang Tan, Jianqiao Ye

► **To cite this version:**

Yong Sheng, Dongmin Yang, Yuanqiang Tan, Jianqiao Ye. Microstructure effects on transverse cracking in composite laminae by DEM. *Composites Science and Technology*, 2010, 70 (14), pp.2093. 10.1016/j.compscitech.2010.08.006 . hal-00682258

HAL Id: hal-00682258

<https://hal.science/hal-00682258>

Submitted on 24 Mar 2012

HAL is a multi-disciplinary open access archive for the deposit and dissemination of scientific research documents, whether they are published or not. The documents may come from teaching and research institutions in France or abroad, or from public or private research centers.

L'archive ouverte pluridisciplinaire **HAL**, est destinée au dépôt et à la diffusion de documents scientifiques de niveau recherche, publiés ou non, émanant des établissements d'enseignement et de recherche français ou étrangers, des laboratoires publics ou privés.

Accepted Manuscript

Microstructure effects on transverse cracking in composite laminae by DEM

Yong Sheng, Dongmin Yang, Yuanqiang Tan, Jianqiao Ye

PII: S0266-3538(10)00314-3
DOI: [10.1016/j.compscitech.2010.08.006](https://doi.org/10.1016/j.compscitech.2010.08.006)
Reference: CSTE 4787

To appear in: *Composites Science and Technology*

Received Date: 14 April 2010
Revised Date: 9 August 2010
Accepted Date: 15 August 2010



Please cite this article as: Sheng, Y., Yang, D., Tan, Y., Ye, J., Microstructure effects on transverse cracking in composite laminae by DEM, *Composites Science and Technology* (2010), doi: [10.1016/j.compscitech.2010.08.006](https://doi.org/10.1016/j.compscitech.2010.08.006)

This is a PDF file of an unedited manuscript that has been accepted for publication. As a service to our customers we are providing this early version of the manuscript. The manuscript will undergo copyediting, typesetting, and review of the resulting proof before it is published in its final form. Please note that during the production process errors may be discovered which could affect the content, and all legal disclaimers that apply to the journal pertain.

Microstructure effects on transverse cracking in composite laminae by DEM

Yong Sheng¹, Dongmin Yang¹, Yuanqiang Tan², Jianqiao Ye^{1,*}

1. School of civil engineering, University of Leeds, LS2 9JT, UK

2. School of mechanical engineering, Xiangtan University, Hunan 411105, China

Abstract

A particle discrete element method (DEM) was employed to simulate transverse cracking in laminated fiber reinforced composites. The microstructure of the laminates was modeled by a DEM model using different mechanical constitutive laws and materials parameters for different constituents, i.e., fiber, matrix and fiber/matrix interface. Rectangular, hexagonal and random fiber distributions were simulated to study the effect of fiber distribution on the transverse cracking. The initiation and dynamic propagation of transverse cracking and interfacial debonding were all captured by the DEM simulation, which showed similar patterns to those observed from experiments. The effect of fiber volume fraction was also studied for laminae with randomly distributed fibers. It was found that the distribution and volume fraction of fibers affected not only the transverse cracking path, but also the behavior of matrix plastic deformation and fiber/matrix interface yielding in the material.

Keywords: Discrete element method; Transverse cracking; Debonding; Matrix cracking; Microstructure; Composite laminae.

1. Introduction

The inherent multi-phased microstructure of fiber reinforced composites, e.g. fiber volume fraction, fiber direction and interfacial strength, results in complex failure modes dominated by fracture of constituent elements. The damage evolution and failure mechanism of composites are obviously far more complex than those of monolithic materials due to the interactions of constituents. The complicated nature of failure/damage modes and physical composition of composite materials make the prediction and evaluation of progressive damage a challenging task. It is very important for material design and structural optimization in composite manufacturing to have the predictive capability on the dynamic failure/damage process. For instance, the properties of a laminate depend very much on the properties of its lamina and ply interface; the behavior of each lamina is, in turn, governed by its constituents, i.e. the properties of the fibers, the surrounding matrix, the interface and the relative amount of fibers and matrix in the lamina. When a composite is under external loading, damage, such as delamination, debonding, matrix cracking and fiber breakage, may occur. The

* Corresponding author. Email: j.ye@leeds.ac.uk

accumulation of the damage during the loading process may eventually cause collapse of the whole material. Therefore a study of the damage or failure modes at micro scale with the consideration of microstructure is a more direct approach to predict the mechanical behavior of the composites.

Traditional micromechanical models focused mainly on the analysis of stress field [1-3], or predicting crack propagation using a prescribed failure criterion for composites with small numbers of fibers [4-6]. The ability to cope with inhomogeneity or/and disorder is essential in order to predict the damage process of a composite from micro cracking to catastrophic failure. Transverse cracking, which normally is formed by matrix cracking and fiber/matrix interfacial debonding, is a familiar phenomenon in a lamina or laminated composite when it is subjected to transverse tension. Finite element method (FEM) has been widely used in this analysis on the basis of imposing various failure criteria [7-9]. However, many of these criteria do not have a rigorous physical basis that can be related to the microstructure of composite materials. Furthermore, the stress field that is calculated to meet the failure criteria of a composite is normally obtained by assuming that the material is not damaged. Thus stress redistribution in the material arising from, e.g., strain softening induced by localized damage cannot be taken into account. Some of the FEM models may agree well with experimental results, but it is very difficult for them to explain how the damage starts and develops in a composite during the entire loading process. Therefore, it is very challenging for a conventional continuum mechanics based numerical model to predict the whole dynamical damage/failure process, from matrix cracking initiation to final laminae/laminates collapse.

A fiber reinforced composites can be imaged as discrete fibers being inserted into a continuous matrix and bonded together by the interfaces between them. The discrete fibers interact with each other through the matrix between them. The analysis of the composite can be carried out through the analysis of the interaction of the discrete fibers. Since a large number of fibers are used in a fiber reinforced composite material, the interaction of these fibers was conventionally studied by the Monte-Carlo method [10, 11]. However, the Monte Carlo method cannot take into account the matrix effect, and the numerical results can hardly interpret the experimental investigations. On the other hand, discrete element method (DEM) [12] combined the statistical analysis with the concept of physical bonds from Molecular Dynamics (MD), and offered an intrinsic advantage over other numerical methods in modeling microscopic and multiphased materials. DEM was proposed by Cundall in the context of rock mechanics [12] and has been implemented in many other fields, such as geomaterials [13], granular materials [14], concrete [15], ceramics [16, 17], particle-fluid [18] and particle-gas two phase flow [19]. Kim et al. [20, 21] used DEM to simulate the damage of asphalt concrete which is a typical example of two-phase composite materials. Yang et al [22] used DEM to simulate the dynamic process of microbond test of single fiber reinforced composite with the consideration of matrix cracking as well as fiber/matrix interfacial debonding. Donze et al. [23, 24] simulated the impacts

of rigid spherical nose shaped missiles on concrete beams with reinforcements. The existing studies concluded that DEM could provide unique insight into damage evolution at both micro and macro scales in the process of the dynamic characterization of fracturing. Van Mier et al. [25, 26] used a lattice beam model, which is equivalent to the DEM model using regular particle arrangements, to study the fracture behavior of concrete from micro-cracking initiation and macro-crack failure in both two and three dimensions. Wittel et al. [27, 28] has applied a lattice spring model, which is a simple form of DEM, to simulate ply transverse cracking of cross-ply laminates, in which the nodes represent fibers and the springs with random breaking thresholds represent the disordered matrix. It has been confirmed by the existing studies that DEM is particularly suitable to simulate dynamic instability in crack propagation and the collective behaviour of many interacting cracks. However, the spring models used for the matrix and interface by Wittel et al. [27, 28] are too simple to represent the mechanical properties of real materials and interfaces. Matrix cracking cannot be correctly simulated by this model and, only regular distribution of fibers with a fixed volume fraction can be considered.

In the research presented in this paper, DEM was used to simulate transverse cracking in laminae, including onset and propagation of the matrix cracking and fiber/matrix interface debonding. Composite laminae with regular distributions of fibers were modeled first and the numerical results were compared with the existing experimental results to validate the developed DEM model. The model was then modified to include random distribution of fibers with different fiber volume fractions. Based on the numerical results from the DEM modelling, the effect of microstructure of the composite laminae on the onset and the propagation path of transverse cracking, and the resulting residual damage within the material can be assessed. The DEM model proposed in this paper can be used for the analysis of more complex composite systems, such as cross-ply laminates.

2. Discrete Element Method (DEM)

The particle discrete element method used in this research assumes that the particle elements are rigid spheroids (3D) or discs (2D), and can overlap or detach from each other. The contact forces between any two particles are determined from the overlap and relative movements of the particle pair according to a specified force-displacement law. In 2D DEM, the motion of a particle over a time step Δt is governed by the Newton's second law as below [12, 14]:

$$\text{Translational motion} \quad F_i = m \left(\frac{\Delta v_i}{\Delta t} - g_i \right) \quad (1)$$

$$\text{Rotational motion} \quad M_3 = I \frac{\Delta \omega_3}{\Delta t} \quad (2)$$

where i ($= 1, 2$) denotes, respectively, the x - and y - co-ordinate directions; F_i is the resultant force of the particle; v_i is the translational velocity; m is the mass of the particle; g_i is the body force acceleration vector (e.g., gravity loading); M_3 is the out

of balance moment referred to the out-of-plane axis; w_3 is the rotational velocity about the out-of-plane axis; I is the rotational inertia of the particle; t is time and Δ is the increment. Damping, e.g., local damping or viscous damping, can be added in the DEM model to dissipate the kinetic energy together with particles' frictional sliding, such that a steady-state solution can be obtained more efficiently [29]. Equations (1) and (2) are solved by a finite difference scheme. Both the specified force-displacement law and Newton's second motion law are used in the calculation cycle of the discrete element method.

DEM allows particles to be bonded together at contacts and to separate when the bond strength or energy is exceeded. Therefore it can simulate the motion of individual particles and also the behavior of a bulk material which is formed by assembling many particles through bonds at contacts with different constitutive laws. In a DEM model of bulk material, elementary micro scale particles are assembled to form the bulk material with macroscopic continuum behavior determined only by the dynamic interaction of particles [29, 30]. Unlike the traditional solution using the strain and stress relations, contact properties are the dominating parameters in a DEM solution, combined with size and shape of the particles. Subject to external loading, when the strength or the fracture energy of a bond between particles is exceeded, flow and disaggregation of the particle assembly occur and the bond starts breaking. Consequently, cracks form naturally at micro scale. Hence, damage modes and their interaction emanate as the process of debonding of particles. The way that DEM discretizes a material domain gives the most significant advantage over the traditional continuum methodologies, as dynamic material behavior of composites, crack tip singularities and crack formulation criteria can all be avoided due to the naturally discontinuous representation of composite materials via particle assemblies.

In a DEM model for composite materials, damage initiation and propagation will take place at the particle contacts under the applied load. There is no requirement for additional failure criteria and the damage of different constituents can be taken into account simultaneously. The damage interaction will also be addressed through the dynamic motion of particles and contacts. The simulation results of a DEM model are naturally discrete and collected at microscopic level. The statistical analysis of the DEM results can also reveal material and structural behavior at macro scale by studying the bonds that have been broken or has yielded.

3. DEM Simulation of Laminae under Transverse Tension

3.1 Constitutive models

A DEM model of a solid material is usually constructed by packing discrete particles into an assembly through rectangular, hexagonal or random arrangement. Random arrangement is the most general approach in which the disperse particles are compacted or expanded to reach a dense contacting network, as shown in Fig.1.

Since a lamina is an inhomogeneous material which includes three phases: fiber, matrix and fiber/matrix interface, individual DEM models for each of the three phases are developed and virtual material tests (e.g., tensile and compressive tests) are carried out on all the phases, respectively, before the construction of the whole lamina model. The fiber material is represented by a parallel bond model whose constitutive behavior is illustrated in Fig.2. A parallel bond can be regarded as a set of elastic springs with constant normal and shear stiffness, uniformly distributed over either a circular or rectangular cross-section lying on the contact plane and centered at the contact point. The bond can transmit both forces and moments. A contact softening model which is similar to the cohesive zone model (CZM) [31] in continuum mechanics is used to account for the matrix and fiber/matrix interface. The only difference between these two models is the unloading and reloading paths after yielding, as shown in Fig.3. The contact softening model describes plastic deformation by linearly softening the bond after the contact force reaches the bond strength. In both tension and shearing, the bond strength decreases to zero when the plastic displacement reaches the maximum plastic displacement U_{pmax} that is related to the fracture energy release rate G . The interfacial crack may be classified as mode I, mode II or mixed mode according to the stress field at the crack tip. In order to automatically capture the three fracture models, the maximum plastic displacement U_{pmax} is kept constant, while the normal and shear strengths of the bond are defined individually. Hence, in a two dimensional system, the fracture energy release rate for mode I and mode II are, respectively:

$$G_I = \frac{1}{2} \cdot \sigma_{nmax} \cdot U_{pmax} \quad (3)$$

And

$$G_{II} = \frac{1}{2} \cdot \sigma_{smax} \cdot U_{pmax} \quad (4)$$

In 2D DEM, the contact stresses at the bond are taken as the average stress between the two contacting particles [29], as calculated below:

$$\sigma_{kmax} = \frac{F_c^k}{A} = \frac{F_c^k}{2R\delta} \quad (5)$$

$$R = \frac{1}{2}(R_1 + R_2) \quad (6)$$

Where, R_1 and R_2 are the radii of the two contacting particles, respectively; δ is the dimension in the out-of-plane direction. k is in place of n or s that indicates normal or shear direction, respectively. Under tension or shearing, the bond starts to yield when the contacting force exceeds the strength and eventually breaks when the plastic displacement reaches the maximum plastic displacement U_{pmax} . In the situation of mixed mode fracture, the bond strength F_{max} (in force unit), is calculated from the two strength parameters (i.e. F_c^n and F_c^s , also in force unit) as a function of the current

direction of the contact force. It is assumed that the contact strength varies linearly with the angle, α :

$$F_{max} = \left(1 - \frac{2\alpha}{\pi}\right) \cdot F_c^n + \frac{2\alpha}{\pi} \cdot F_c^s \quad (7)$$

Where α is the angle between the directions of the contact force and the line segment connecting the centers of the two particles. The yielding of the bond in tension is determined by comparing the resultant contact force, i.e.

$$F = \sqrt{(F^n)^2 + (F^s)^2} \quad (8)$$

with the contact strength. The bond yields if the contact force is larger than the contact strength:

$$F > F_{max} \quad (9)$$

The maximum plastic displacement U_{pmax} is calculated from the displacements in the normal and shear directions. In each computation step, the increments of normal and shear plastic deformation, which are denoted by Δ , are subjected to a consistence condition of:

$$(\Delta U_p)^2 = (\Delta U_p^n)^2 + (\Delta U_p^s)^2$$

(10)

$$\frac{\Delta U_p^n}{\Delta U_p^s} = \tan \alpha$$

(11)

When the plastic displacement reaches U_{pmax} ,

$$\Sigma |\Delta U_p| \rightarrow U_{pmax}$$

(12)

The fracture energy release rate can be calculated as:

$$G = \frac{1}{2} \cdot \sigma_n \cdot U_p^n + \frac{1}{2} \cdot \sigma_s \cdot U_p^s = \frac{1}{2} \cdot \sigma_n \cdot \Sigma |\Delta U_p^n| + \frac{1}{2} \cdot \sigma_s \cdot \Sigma |\Delta U_p^s|$$

(13)

In which σ_n and σ_s are the normal and shear stresses of the bond when yield occurs, i.e., equations (8) and (9) are satisfied. For the mixed mode, the fracture energy release rate is somewhere between the rates of the two single fracture modes.

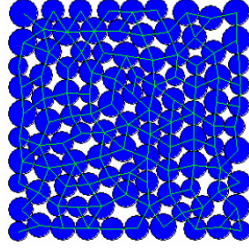


Fig.1 Random arrangement of particles

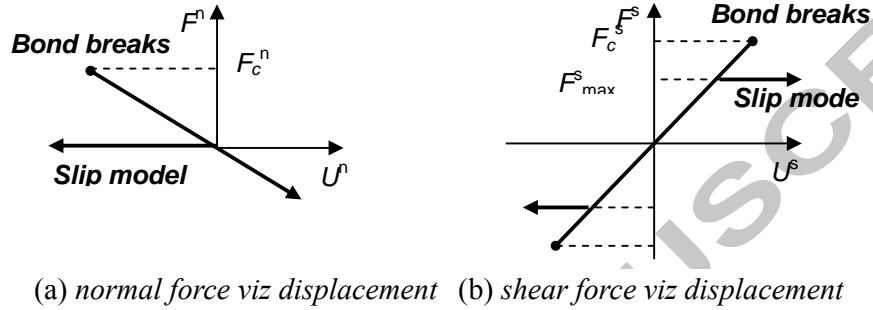


Fig.2 Constitutive behavior of the parallel bond at contact

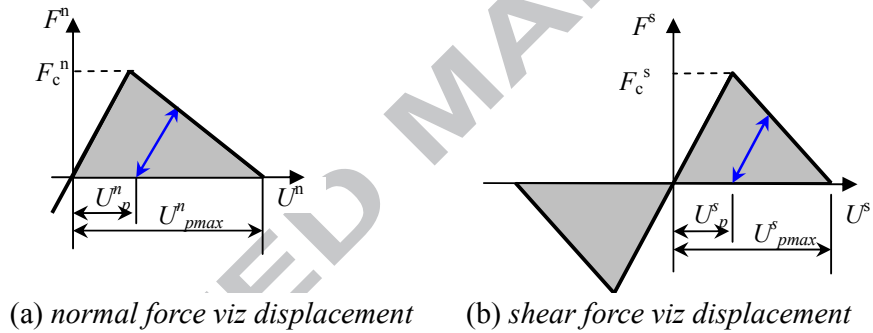


Fig.3 Constitutive behavior of contact softening model

3.2 Convergence study

Since displacement loading is used in this research, including the fiber, matrix and the laminae tensile tests shown in the following sections, the influence of loading velocities on the solutions is studied by comparing the stress-strain curves obtained from a parallel bond model subject to different tensile loading velocities, as shown in Fig.4. It is found that for all loading velocities below 0.1m/s, the tests lead to almost identical results. Therefore, $v=0.1\text{m/s}$ is chosen as the loading velocity in all subsequent cases to achieve the quasi-static conditions.

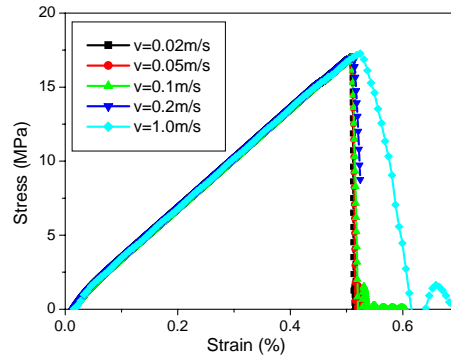


Fig.4 Convergence of loading velocities for quasi-static simulation

After the convergence study on velocity, a Double Cantilever Beam (DCB) virtual test [32, 33], which has been widely applied to investigate interface strength, is conducted by the 2D DEM model with square arrangement of particles. The test is to assess the effect of particle size on the failure of the contact softening model. The model consists of two identical material layers [34], as shown in Fig.5, each of which is further divided into 2 plies. The contacts between the particles within each layer are modeled by the parallel bond, while the interface between the two layers is represented by the contact softening model. The length of the plies is 45mm and the thickness is 3mm. An initial interfacial crack of 20mm length from the left end of the beam is generated by removing the interfacial bonds between the two layers. The right end of the beam is fixed. The loading is applied by assigning a constant separation velocity in the vertical direction to the particles at the left ends of the two layers, which results in a variable opening end displacement. Different particle sizes are used in this simulation to examine their effect on the interfacial fracture and the results are illustrated in Fig.6. It is found that the model shows good convergence and numerical results agree very well with the theoretical solution by the J -integral theory in [34], though the results for $R=0.75\text{mm}$ are slightly distanced from the group, which is due to the fact that for this case only one ply of particles is used in each layer. The good convergence of the contact softening model indicates that the influence of particle size on the model is not significant as long as the particle size is sufficiently small and the model can be adopted to simulate the fracture of matrix and fiber/matrix interface.

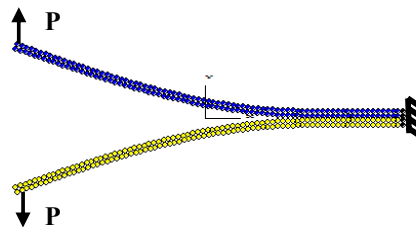


Fig.5 DEM model of DCB test

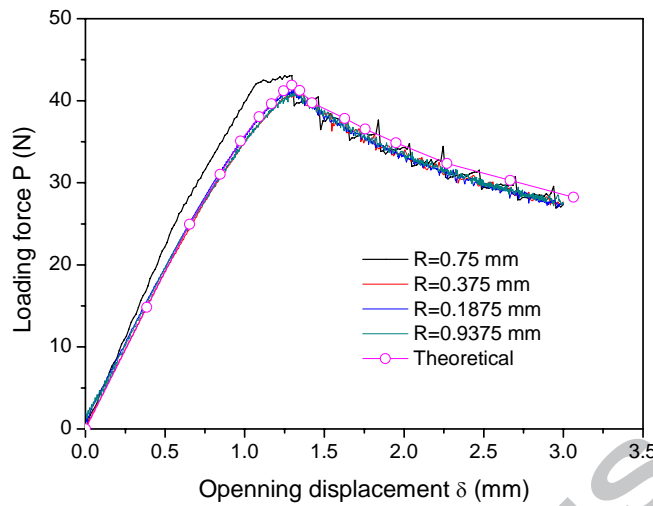


Fig.6 Convergence of particle sizes in the DEM simulations of DCB test

3.2 DEM simulations

Glass fiber reinforced composites are taken as examples in this paper, where the glass fiber and the epoxy matrix are both considered as linear isotropic materials. The matrix, the fiber and then the composites are all generated using the particle assembly model [16, 29]. Particles with a radius between R_{min} and R_{max} are randomly generated according to the normal distribution law in a cell. Since the particles are randomly packed, it is not realistic to derive directly a rigorous and theoretical relationship between the micro properties and the macro mechanical properties, such as between particle stiffness, contact stiffness and contact strength and the elastic modulus, Poisson's ratio and tensile strength. However, each of the macro mechanical properties is related to one or several of the micro parameters. For instance, the elastic modulus is only related to the particle and contact stiffness, but not the contact strength and particle size. Based on this observation, virtual simulation tests are usually carried out to determine the micro properties in order to obtain the required macro mechanical properties. Virtual tensile tests on the DEM model of the glass fiber and the epoxy matrix are carried out to validate the main mechanical properties, as listed in Table.1. Figures 7 and 8 show the respective strain-stress relationships, where both the longitudinal and transverse strains are recorded against the applied tensile load. The parameters in the above calibrated DEM models are then incorporated in the laminae model satued in the following sections.

Table 1 Material properties of the DEM model

Fiber modulus (glass)	60 GPa
Fiber Poisson's ratio	0.23
Fiber radius	25 μm

Matrix modulus (epoxy)	2.8 GPa
Matrix Poisson's ratio	0.35
Matrix yield stress	62 MPa
Interface modulus	3.3 GPa
Interfacial bond strength (tensile)	50 MPa
Interfacial bond strength (shear)	50 MPa
Interface fracture energy release rate (mode I or mode II)	100 J/m ²

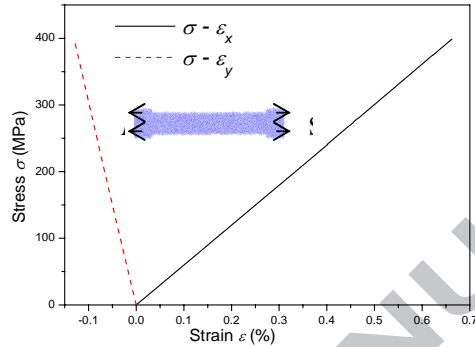


Fig.7 Stress-strain curve in DEM simulation of fiber tensile test

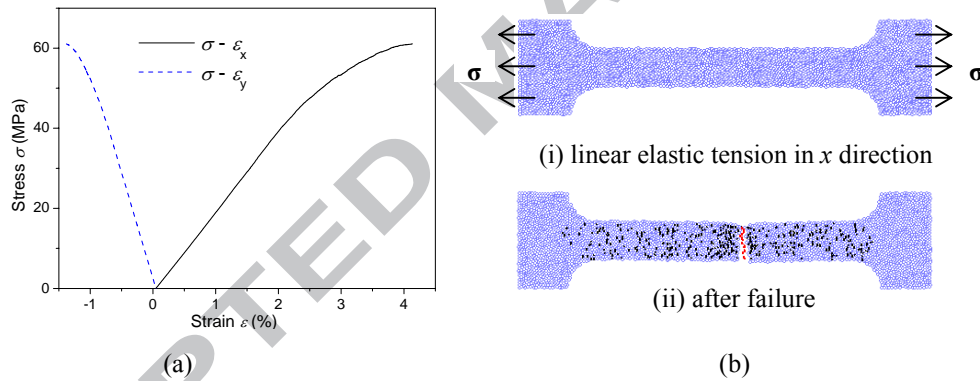


Fig.8 DEM simulation of matrix tensile test

(Black and red lines describe matrix plastic deformation and matrix failure in b(ii), respectively)

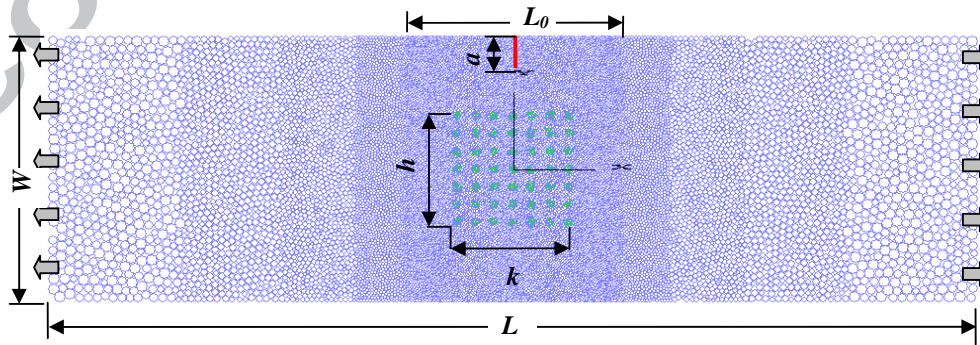
Specimen height: $W=1.5$ mmSpecimen length: $L=5$ mmInitial specimen length: $L_0=1.0$ mmInitial crack length: $a=100$ μm Square height: $h=650$ μm Square length: $k=650$ μm

Fig.9 DEM model of laminae with multiple particle sizes

In this study transverse cracking of a glass/epoxy lamina under tensile loading, as shown in Fig.9, is studied, where three types of fiber distribution and three fiber volume fractions are considered. The interface strength is smaller than that of the matrix, with both the tensile and shear strength being 50 MPa, and the interface fracture energy is chosen as 100 J/m². A large length-to- depth ratio is used to eliminate the far field loading effect. The particles with a minimum radius of $R_{min}=5 \mu\text{m}$ ($R_{max}=1.5R_{min}$) are generated first within a rectangular square of 1.5 mm \times 1.0 mm in the middle of the specimen, where the fibers are inserted, to represent the composite. The central part is then extended to the both sides by a sequence of four rectangular assemblies composed of larger matrix particles. The final size of the model is 1.5 mm \times 5 mm. The fibers are located in a small square area of 650 μm \times 650 μm in the middle of the specimen in order to create a fiber reinforced composite laminae. An initial crack of length a was created in the matrix at the top of the mid-span by deleting the corresponding particle elements. This is used to ensure that a transverse crack would propagate towards the fiber reinforced area to simulate the experimental study in [35]. A constant displacement loading with a velocity of 0.1m/s is applied at the both ends of the specimen.

In order to study the effect of fiber distribution on the transverse cracking, rectangular, hexagonal and random distributions of 49 fibers are used in the DEM models as shown in Fig.10. The numerical results are compared with the experimental observations of transverse cracking path in Fig.11. As the load applied at the two ends increases, matrix cracking, which is initiated from the preset crack, propagates into the interior area of the material and subsequently interacts with interfacial debonding. The cracks finally propagate through the entire matrix as illustrated in Fig.10 (i) and Fig.10 (ii). In all of the three cases of fiber distribution, when the force between two matrix particles exceeds the bond strength of the material, the matrix exhibits plastic deformation (represented by the black lines in Fig.10) and finally breaks when the fracture energy is reached. At this moment, the black lines are replaced by the red lines in Fig.10 to show the formation of cracks. Similarly, fiber/matrix interface started to yield when its strength is exceeded (represented by the brown lines in Fig.10), and debonding occurs when its strength is softened to zero, represented then also by the red lines. From Fig.10, it can be seen that the entire dynamic damage process of the initiation and propagation of cracking can be naturally simulated by the DEM model.

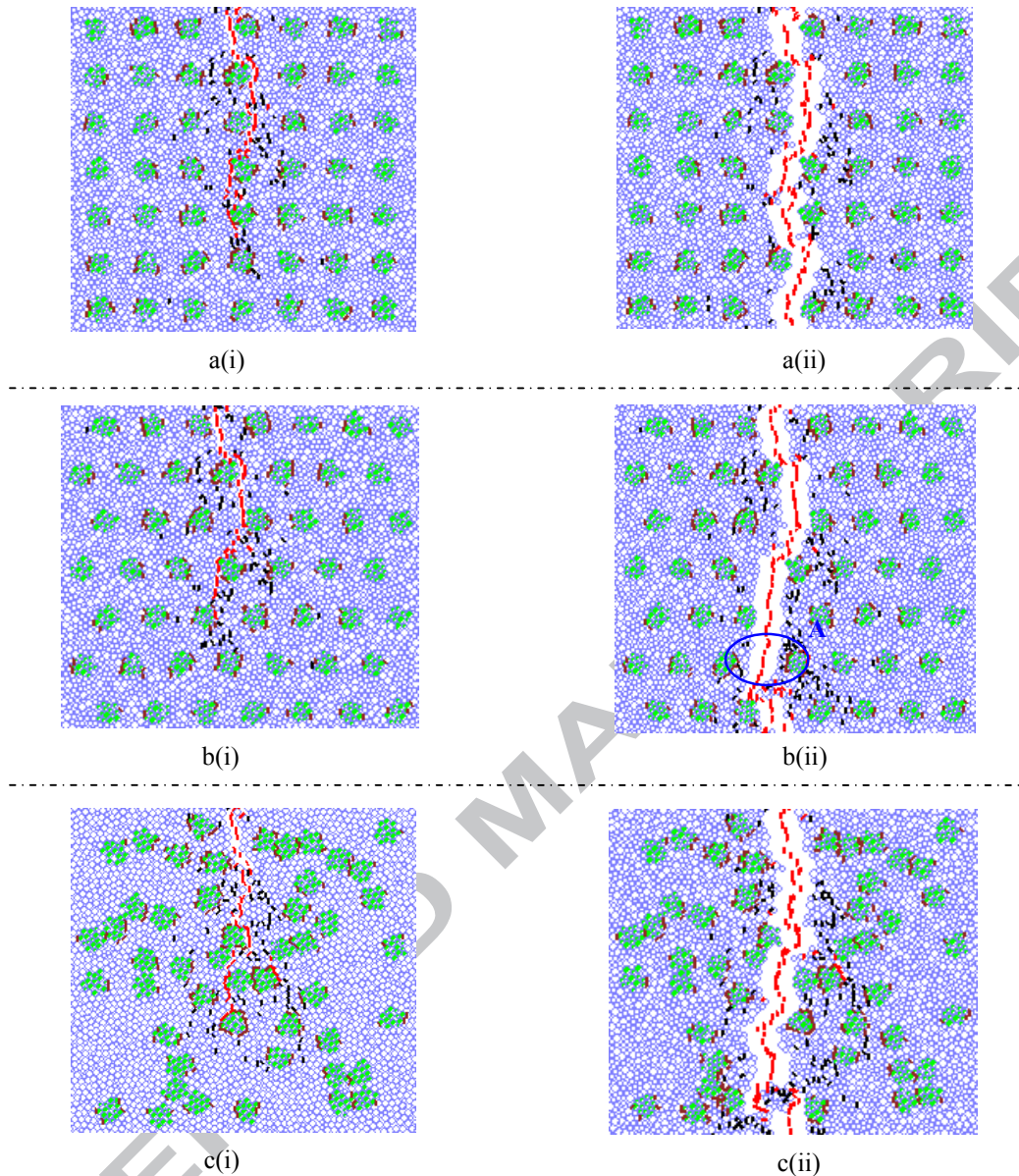


Fig.10 DEM dynamic simulation of transverse cracking in laminae ('a', 'b' and 'c' represent rectangular, hexagonal and random distribution of fibers, respectively; Red, black and brown lines describe transverse cracking, matrix plastic deformation and interface yield, respectively.)

4. Results and Discussions

It can be found from the DEM results that for all the three fiber distributions the transverse cracks propagate through the middle part of the fiber reinforced area, and the crack development is altered and/or interrupted by fibers and fiber/matrix interfaces, resulting in a zigzag path, as shown in Fig.10 (ii). Plastic deformation of the matrix and fiber/matrix interfacial yielding can be observed on both sides of the transverse cracks, but more severe plastic deformation of the matrix and fiber/matrix interfacial yielding are found in the vicinity of the transverse crack.

In the laminae with rectangular distribution of fibers, interfacial debonding always occurs when the crack propagates toward the fiber/matrix interface, though some of the debondings occurs on the left hand side of a fiber, while others takes place on the right hand side. A similar phenomenon has been recorded in the experimental investigation [35], as shown in Fig.11(a).

In the laminae with hexagonal arrangement of fibers, the transverse cracking path is slightly different. It joins the fiber/matrix interfacial debondings as well as penetrates through the matrix between two horizontally neighboring fibers, and directly propagates forward, as highlighted in zone (A) of Fig.10 b(ii) and (A') of Fig.11 (b). The concentrated matrix plastic deformation and interface yielding are then formed on both sides of the crack, as can be seen in Fig.10 b(ii), which dissipates the extra energy that is needed to debond the interfaces. The transverse crack selects the weaker matrix in plastic deformation instead of the fiber/matrix interfaces as the propagation route.

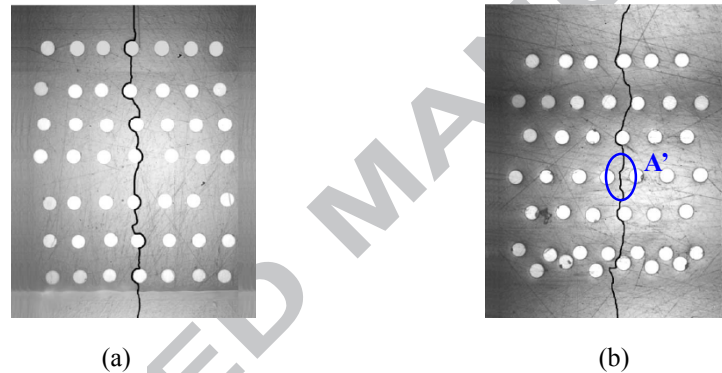


Fig.11 Experimental observation of cracks in laminae with different arrangement of fibers in [35]:
(a) rectangular; (b) hexagonal

The propagation of transverse cracking in randomly distributed fiber reinforced laminae is much more complex in reality, and is successfully simulated by the DEM model without introducing any assumptions on how the crack should propagate, as shown by the numerical results in Fig.10c. The direction of the transverse cracking is more or less random but generally followed the middle line of the specimen. It is also a mixture of joining interfacial debonding and matrix cracking.

It is evident that the DEM results have provided a unique insight of the microscopic damage within the composite laminae. One of the unique features of the DEM model is that the dynamic simulation can record all the damage accumulated during the loading process. From these records, it can be found that the distribution of fibers not only affects the transverse cracking path, but also causes different residual damage, such as matrix plastic deformation and fiber/matrix interfacial yielding in the material. Fig.12 presents a statistic summary of the damage accumulated in the loading process.

In the laminae with rectangular fiber distributions, the number of residual damage, in terms of the total number of the particle contacts exhibiting either matrix plastic deformation or fiber/matrix interface yielding, is smaller than that with hexagonal or randomly distributed fibers. This suggests that laminae with rectangular distribution of fibers can offer better residual mechanical properties. This is due to the fact that a rectangular distribution of fibers can offer more uniform stress distribution within the laminae, resulting in a lower level of stress concentration, and then a reduction of plastic deformation and fiber/matrix interface debonding.

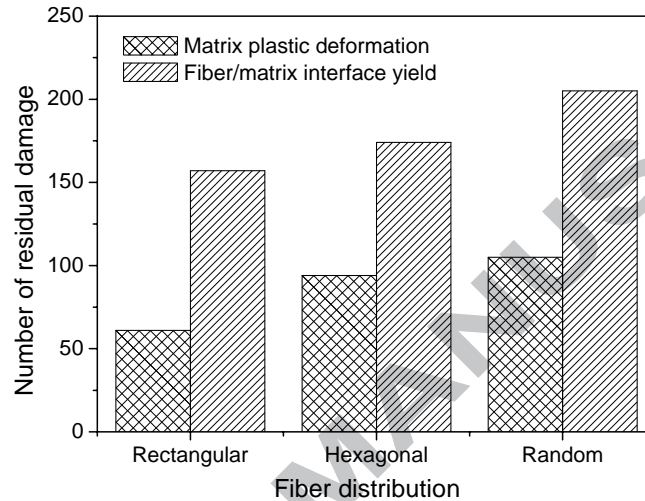


Fig.12 Residual damage in laminae with different fiber distributions

For randomly distributed fiber reinforcement, Figures 13 and 14 show the results obtained by the DEM model with different fiber volume fractions. In the laminae with lower fiber volume fractions, a more diverted transverse cracking path is observed, probably due to the fact that more matrix material between two neighboring fibers has left more freedom for the transverse crack to pass through, which creates a relatively less uniform path. When the fiber volume fraction is higher, the propagation of the transverse cracking is largely guided by fiber/matrix interfacial debonding, and therefore, the path of transverse cracking is more direct, resulting in a much smoother crack.

Also in the case of random distribution of fibers, it can be found that the total fiber/matrix interfacial yielding increases, while the number of matrix plastic deformation decreases, with the increase of the fiber volume fraction, as illustrated in Fig.14. This is due to the reduction of matrix volume and average distance between two neighboring fibers, making the interfaces much easier to yield.

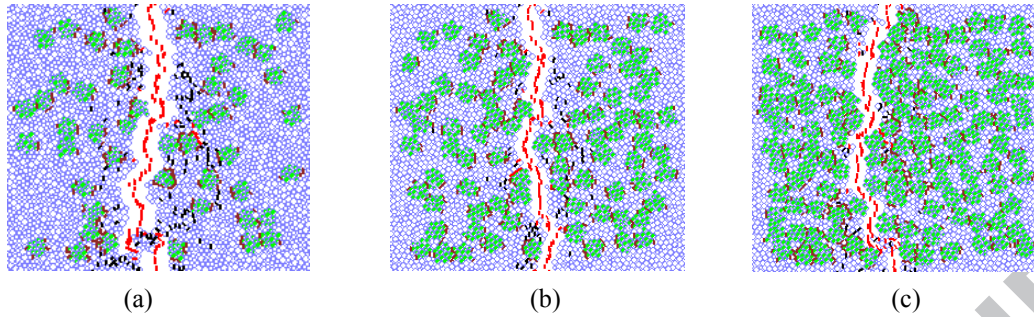


Fig.13 Transverse cracking in laminae with random fiber distribution and different fiber volume fractions:
(a) 23.2%, (b) 37.6% and (c) 56.2%.

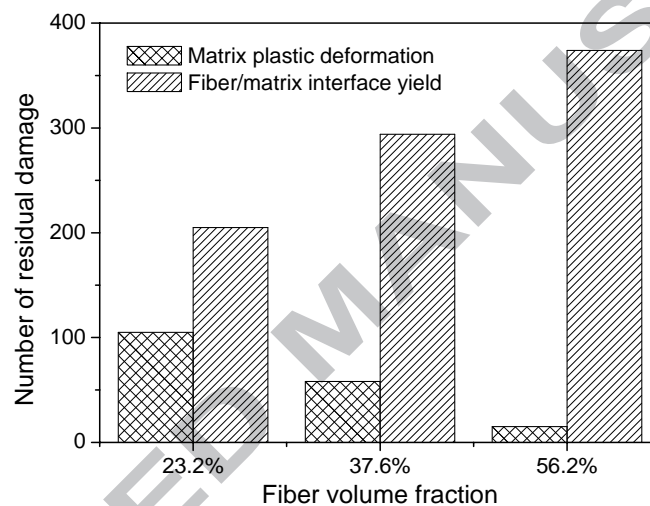


Fig.14 Residual damage in laminae with different fiber volume fractions

5. Conclusions

Discrete element method (DEM) has been employed to simulate transverse cracking in composite laminae, due to its intrinsic advantages in modeling microscopic damage and fracturing in multiphased materials. Three types of fiber distributions, i.e., rectangular, hexagonal and random distributions, have been simulated to study the effect of fiber distribution on the transverse cracking. The initiation as well as dynamic propagation of transverse cracking has been captured by the DEM model, showing good agreement to the experimental observations. Furthermore, the DEM simulations have provided unique insights of the microscopic cracking and damage in forms of matrix plastic deformation and fiber/matrix interface yielding. The effect of fiber volume fraction was also studied by using different fractions in the DEM modeling for randomly distributed fibers.

It is a unique feature of the DEM that allows a quantitative study of the residual microscopic damage within a fractured material. This has led to the findings that the

distribution and volume fraction of fibers not only affect the transverse cracking path, but also the mechanical behaviors of the material through the populations of the residual matrix plastic deformation and fiber/matrix interfacial yielding.

It can be concluded that the DEM developed in this paper is particularly suitable for the modeling of complex multi scale damage and cracking in multiphase composite materials, and can be further modified to include thermal effect and applied to model more complex composite systems in the future, such as cross-ply laminates.

6. Acknowledgement

The authors wish to thank Professor N L McCartney, the National Physical Laboratory, for reviewing an early version of the manuscript and providing detailed criticism and comments. The second author would like to acknowledge the ORSAS scholarship and the University of Leeds studentship for the financial support of his PhD study. The third author would like to thank the NSFC of China for the financial support of this collaboration research under the grant of No.50875224.

Reference

- [1] Asp LE, Berglund LA, Talreja R. Prediction of matrix-initiated transverse failure in polymer composites. *Composites Science and Technology*. 1996;56(9):1089-1097.
- [2] Asp LE, Berglund LA, Talreja R. Effects of fiber and interphase on matrix-initiated transverse failure in polymer composites. *Composites Science and Technology*. 1996;56(6):657-665.
- [3] Trias D, Costa J, Mayugo JA, Hurtado JE. Random models versus periodic models for fibre reinforced composites. *Computational Materials Science*. 2006;38(2):316-324.
- [4] Zhang X, Liu H-Y, Mai Y-W. Effects of fibre debonding and sliding on the fracture behaviour of fibre-reinforced composites. *Composites Part A: Applied Science and Manufacturing*. 2004;35(11):1313-1323.
- [5] Rao GVG, Mahajan P, Bhatnagar N. Micro-mechanical modeling of machining of FRP composites - Cutting force analysis. *Composites Science and Technology*. 2007;67(3-4):579-593.
- [6] Vejen N, Pyrz R. Transverse crack growth in glass/epoxy composites with exactly positioned long fibres. Part II: numerical. *Composites Part B: Engineering*. 2002;33(4):279-290.
- [7] Berthelot JM, El Mahi A, Leblond P. Transverse cracking of cross-ply laminates: Part 2. Progressive widthwise cracking. *Composites Part A: Applied Science and Manufacturing*. 1996;27(10):1003-1010.
- [8] Sjögren BA, Berglund LA. The effects of matrix and interface on damage in GRP cross-ply laminates. *Composites Science and Technology*. 2000;60(1):9-21.

- [9] Okabe T, Nishikawa M, Takeda N. Numerical modeling of progressive damage in fiber reinforced plastic cross-ply laminates. *Composites Science and Technology*. 2008;68(10-11):2282-2289.
- [10] Okabe T, Sekine H, Noda J, Nishikawa M, Takeda N. Characterization of tensile damage and strength in GFRP cross-ply laminates. *Materials Science and Engineering A*. 2004;383(2):381-389.
- [11] Mishnaevsky L, Brondsted P. Statistical modelling of compression and fatigue damage of unidirectional fiber reinforced composites. *Composites Science and Technology*. 2009;69(3-4):477-484.
- [12] Cundall PA, Strack ODL. A discrete numerical model for granular assemblies. *Géotechnique*. 1979;29(1):47-65.
- [13] Hunt SP, Meyers AG, Louchnikov V. Modelling the Kaiser effect and deformation rate analysis in sandstone using the discrete element method. *Computers and Geotechnics*. 2006;30:611-621.
- [14] Sheng Y, Lawrence CJ, Briscoe B, Thornton C. Numerical studies of uniaxial powder compaction process by 3D DEM. *Engineering Computations: International Journal for Computer-Aided Engineering*. 2004;21(2-3):304-317.
- [15] Frédéric SH, Donzé V, Daudeville L. Discrete element modeling of concrete submitted to dynamic loading at high strain rates. *Computers & Structures*. 2004;82:2509-2524.
- [16] Tan Y, Yang D, Sheng Y. Study of polycrystalline Al₂O₃ machining cracks using discrete element method. *International Journal of Machine Tools and Manufacture*. 2008;48(9):975-982.
- [17] Tan YQ, Yang DM, Sheng Y. Discrete element method (DEM) modeling of fracture and damage in the machining process of polycrystalline SiC. *Journal of the European Ceramic Society*. 2009;29(6):1029-1037.
- [18] Feng YT, Han K, Owen DRJ. Coupled lattice Boltzmann method and discrete element modelling of particle transport in turbulent fluid flows: Computational issues. *International Journal for Numerical Methods in Engineering*. 2007;72:1111-1134.
- [19] Chu KW, Wang B, Yu AB, Vince A. CFD-DEM modelling of multiphase flow in dense medium cyclones. *Powder Technology*. 2009;193(3):235-247.
- [20] Kim H, Wagoner MP, Buttlar WG. Simulation of fracture behavior in asphalt concrete using a heterogeneous cohesive zone discrete element model. *Journal of Materials in Civil Engineering*. 2008;20(8):552-563.
- [21] Kim H, Wagoner MP, Buttlar WG. Numerical fracture analysis on the specimen size dependency of asphalt concrete using a cohesive softening model. *Construction and Building Materials*. 2009;23(5):2112-2120.
- [22] Yang D, Sheng Y, Ye J, Tan Y. Discrete element modeling of the microbond test of fiber reinforced composite. *Computational Materials Science*. 49(2):253-259.

- [23] Magnier SA, Donze FV. Numerical simulations of impacts using a discrete element method. *Mechanics of Cohesive-Frictional Materials*. 1998;3(3):257-276.
- [24] Shiu WJ, Donze FV, Daudeville L. Penetration prediction of missiles with different nose shapes by the discrete element numerical approach. *Computers & Structures*. 2008;86(21-22):2079-2086.
- [25] Van Mier JGM, Van Vliet MRA. Influence of microstructure of concrete on size/scale effects in tensile fracture. *Engineering Fracture Mechanics*. 2003;70(16):2281-2306.
- [26] van Mier JGM, Man HK. Some Notes on Microcracking, Softening, Localization, and Size Effects. *International Journal of Damage Mechanics*. 2009;18(3):283-309.
- [27] Wittel FK, Schulte-Fischedick J, Kun F, Kröplin B-H, Frieß M. Discrete element simulation of transverse cracking during the pyrolysis of carbon fibre reinforced plastics to carbon/carbon composites. *Computational Materials Science*. 2003;28(1):1-15.
- [28] Wittel FK, Kun F, Kröplin B-H, Herrmann HJ. A study of transverse ply cracking using a discrete element method. *Computational Materials Science*. 2003;28(3-4):608-619.
- [29] Itasca Consulting Group Inc. PFC2D (particle flow code in 2-dimensions), Version 3.10, User Manual. Minneapolis, Minnesota. 2004.
- [30] Potyondy DO, Cundall PA. A bonded-particle model for rock. *International Journal of Rock Mechanics and Mining Sciences*. 2004;41(8):1329-1364.
- [31] Hu N, Zemba Y, Fukunaga H, Wang HH, Elmarakbi AM. Stable numerical simulations of propagations of complex damages in composite structures under transverse loads. *Composites Science and Technology*. 2007;67(3-4):752-765.
- [32] Meo M, Thieulot E. Delamination modelling in a double cantilever beam. *Composite Structures*. 2005;71(3-4):429-434.
- [33] Li S, Thouless MD, Waas AM, Schroeder JA, Zavattieri PD. Use of mode-I cohesive-zone models to describe the fracture of an adhesively-bonded polymer-matrix composite. *Composites Science and Technology*. 2005;65(2):281-293.
- [34] Ouyang ZY, Li GQ. Local Damage Evolution of Double Cantilever Beam Specimens During Crack Initiation Process: A Natural Boundary Condition Based Method. *Journal of Applied Mechanics-Transactions of the Asme*. 2009;76(5).
- [35] Vejen N, Pyrz R. Transverse crack growth in glass/epoxy composites with exactly positioned long fibres. Part I: experimental. *Composites Part B: Engineering*. 2001;32(7):557-564.